

Undecabenzo[7]superhelicene: a helical nanographene ribbon as CPL emitter

Carlos M. Cruz,^[a] Silvia Castro-Fernández,^[a] Ermelinda Maçõas,^[b] Juan M. Cuerva^[a] and Araceli G. Campaña^{*[a]}

Abstract: We report the synthesis and characterization of an enantiopure superhelicene nanographene constituted by two saddle-shaped and one planar hexabenzocoronene (HBC) units arranged in a helicoidal shape. This is, to the best of our knowledge, the first undecabenzo[7]carbohelicene, i.e., the first fully π -extended [7]helicene. Racemic resolution allowed its chiroptical properties analysis revealing dissymmetry factors in the range of 2×10^{-3} both in the absorption and in the emission measurements. Remarkably, non-linear photophysical analysis showed two-photon absorption cross-section of 870 GM at 800 nm and a perfect overlapping between linear, non-linear and chiral emission.

Theoretical and experimental studies have demonstrated that folding graphene induces changes in its original characteristics, tuning the electronic transport^[1] and the thermal properties.^[2] In this sense, the synthesis of curved saddle nanographenes is receiving major attention in recent years in the search of new geometries and optoelectronic properties in carbon nanostructures.^[3] Thus, considerable progress has been made on the bench-top synthesis of nanographenes containing seven- and eight-membered carbocycles.^[4]

Recent works also show that graphene helicoids (GH), like nanosprings or nanosolenoids, could exhibit superior properties than multilayer graphene (MLG) of similar size in terms of controlling thermal conductivity,^[5] tensile^[6] or magnetic properties.^[7] Helical twisted nanographenes are promising candidates also in the field of chiral electronics and very relevant recent examples have been presented on chiral enantiopure nanographenes showing inherent chiroptical properties and electronic responses of interest in a variety of applications.^[8] Regarding the chiroptical properties, circularly polarized luminescence (CPL)^[9] is gaining ground because of the many applications envisioned for compounds with this sort of emission capabilities, as molecular switches,^[10] ratiometric probes,^[11] or light-emitting devices.^[12] Therefore, inducing chiroptical properties, such as CPL, in graphene-related materials would afford new candidates of great potential for applications in the area of organic electronic materials.^[12a]

In this communication, we present the synthesis, characterization and optical properties of the first fully π -extended [7]carbohelicene as a constituent of a chiral nanographene **1** (Figure 1). In the final molecule, a [7]carbohelicene is fully surrounding by fused benzene rings leading to the first undecabenzo[7]carbohelicene.^[13] Compound **1** is a HBC-based helicene,^[8c,d] a new member of the recently coined family of “superhelicenes” and the first one constituted by three HBC-like units: two heptagon containing saddle-shaped HBCs at the edges and one central planar HBC unit. This super[7]helicene constitutes a nanographene helicoid that is a primary substructure of a graphenic Riemann surface^[14] with remarkable non-linear and chiroptical properties.

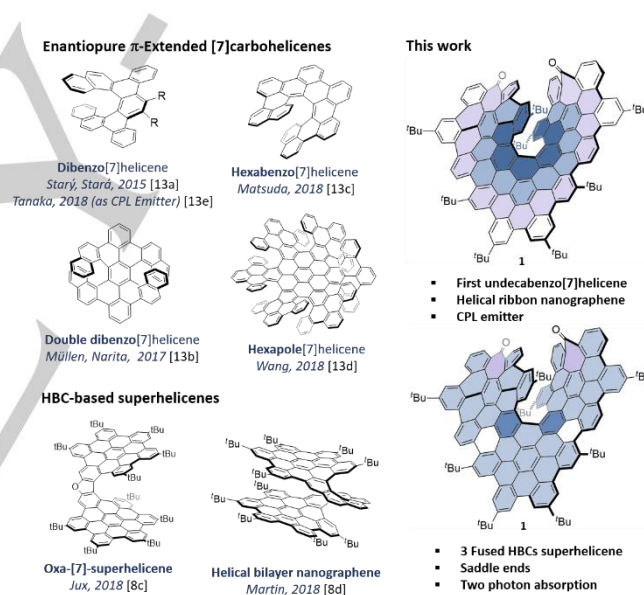


Figure 1. Background and novel structural features of compound **1**

Looking for a straightforward synthesis (Scheme 1A), we took advantage of our described methodology for the preparation of heptagon-containing hexaphenylbenzene **2** by a Co-catalyzed alkyne cyclotrimerization reaction.^[3g] Treatment of **2** with the combination DDQ/TfOH led to heptagon containing HBC **4**. Both **2** and **4** were linked by an acetylene unit through two consecutive Sonogashira couplings leading to **5**. The third unit of hexaphenylbenzene was created in the subsequent step via Diels-Alder reaction with 2,3,4,5-tetrakis(*p*-*tert*-butyl-phenyl)-cyclopentadienone. Final oxidative cyclodehydrogenation reaction created the two new units of HBCs in a single step, leading to helical nanographene strip **1** as major product.^[15] The unequivocal assignment of the structure of **1** was addressed by means of ¹H NMR (Scheme 1B), ¹³C NMR, 2D-NMR (HSQC, COSY) and 1D-ROESY (see SI for details).^[16] Besides, HRMS

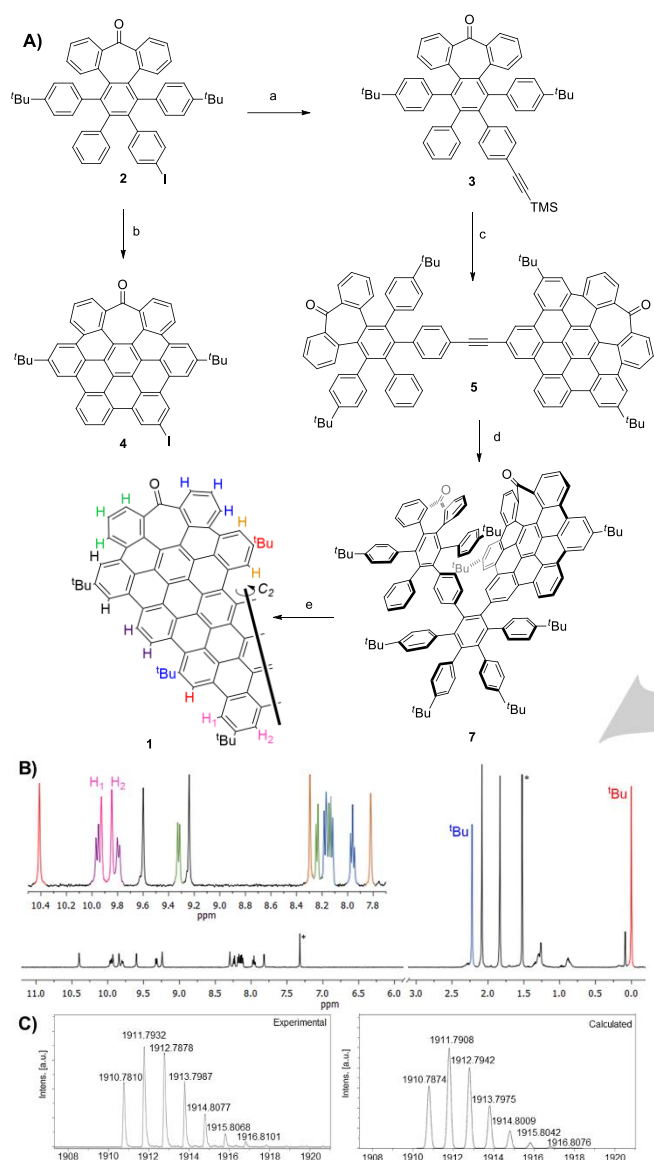
[a] C. M. Cruz, Dr. S. Castro-Fernández, Prof. J. M. Cuerva, Dr. A. G. Campaña
Departamento de Química Orgánica, Facultad de Ciencias
Universidad de Granada
Avda. Fuentenueva, s/n, E-18071 Granada, Spain
E-mail: aracelg@ugr.es

[b] Dr. E. Maçõas
Centro de Química Estrutural and Institute of Nanoscience and
Nanotechnology (IN), Instituto Superior Técnico
University of Lisbon
Av. Rovisco Pais, 1, 1049-001 Lisboa, Portugal

Supporting information for this article is given via a link at the end of the document.

COMMUNICATION

measurements by MALDI-TOF, showed only one peak with the mass and the isotopic distribution pattern in good agreement with the calculated one for **1** (Scheme 1C).



Scheme 1. (A) Synthetic route yielding **1**. Reagents and conditions: a) trimethylsilylacetylene, PdCl₂(PPh₃)₂, CuI, NEt₃, THF, RT, 16 h, 99%; b) DDQ, CF₃SO₃H, CH₂Cl₂, 0 °C, 10 min, 86%; c) **4**, PdCl₂(PPh₃)₂, CuI, NEt₃, DBU, THF, H₂O, reflux, 24 h, 84%; d) **6**: 2,3,4,5-tetrakis(*p*-*tert*-butyl-phenyl)-cyclopentadienone, Ph₂O, reflux, 10 h, 75%; e) DDQ, CF₃SO₃H, CH₂Cl₂, 0 °C, 10 min, 7%. (B) ¹H NMR spectrum of **1** (500 MHz, CD₂Cl₂, 293K), *residual solvent peak. (C) Isotopic distribution HR-MS (MALDI-TOF) of **1**.

According to DFT calculations (CAMB3LYP/6-31G(d,p)), the 39-ring π -surface of **1** forms a ribbon of around 3 nm length and 1 nm width, fully arranged in a spiral shape around a central [7]carbohelicene (Figure 2). In the most stable geometry of (*M*)-**1** the helix completes a whole turn over itself as the first and last [7]helicene rings are placed over each other (Figure 2, top right, green). The *t*-butyl groups at the ends of the [7]helicene stand

over the π -surfaces of the opposite curved-HBC areas which is reflected on their very low ¹H-NMR chemical shift. The angle between the two planes of the terminal rings is 25.3 °, shorter than that of the single [7]helicene (32.8°) and the torsion angles along helical inner rim are ϕ =30.0, 29.0, 21.7, 27.9 and 30.2° with a mean value of 27.8 °, which is larger than that of the [7]helicene (22°).^[17] The two ends of the helical ribbon present a saddle-curvature derived from the inclusion of seven-membered carbocycles. Thus, the two ketones face each other pointing inwards giving a good packing of the curved π -surfaces accommodating the seven-membered rings (Figure 2, bottom, right). The C–C distances of the seven-membered ring measured on the optimized structure are the typical for a cyclohepta-2,4,6-trienone.

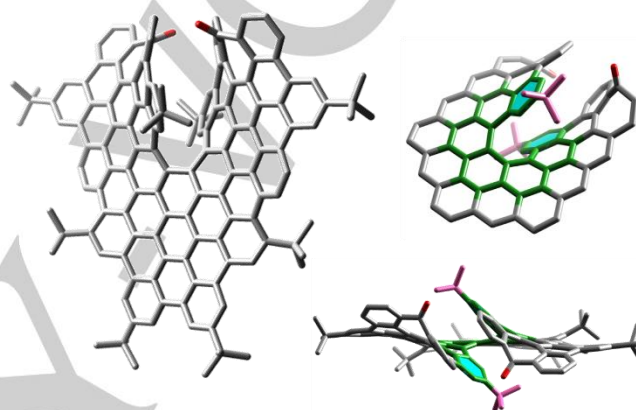


Figure 2. DFT (CAMB3LYP/6-31G(d,p)) optimized structure of (*M*)-**1**. Left: side view. Right: frontal view (bottom) and undecabenzo[7]helicene fragment (top).

Noteworthy, **1** presents good solubility in common organic solvents such as chloroform, dichloromethane or hexane (up to 8.33 mg mL⁻¹ in CHCl₃). Helical nanographene **1** shows orange color in CH₂Cl₂ solution. Thus, its UV-Vis spectrum recorded in the 300-800 nm region presents a broad absorption band centered at 472 nm, with a maxima also at 510 nm. The longest wavelength absorption band is centered at 580 nm extending up to 600 nm (Figure 3, bottom, blue). This band is dominated by the transitions from the HOMO-1, HOMO, to the LUMO and LUMO+1 with the HOMO and LUMO involving mostly the central planar HBC and the [7]helicene moiety and the HOMO-1 and LUMO+1 extending over the distorted HBCs at the two edges. The molar absorptivity coefficient was estimated as 1.6 × 10⁵ M⁻¹cm⁻¹ (at λ_{\max} = 472 nm). The vibronic progression might also contribute to the absorption band, as it is typical in aromatic systems.

Compound **1** exhibited notably intense orange-red fluorescence when irradiated with UV light, with a maximum centered at 610 nm (Figure 3, bottom, navy blue). The fluorescence quantum yield (ϕ_F) is 9.8% in CH₂Cl₂ which is among the highest described for π -extended [7]helicenes^[13] and represents a notably 4.7-fold increase in comparison with the one described for heptahelicene (ϕ_F = 2.1%).^[18] The excitation independent emission and the overlapping between the absorption and excitation spectra confirmed the purity of the sample and the absence of aggregates up to 10⁻⁵ M concentration. The average emission lifetime is τ = 18.0 ± 2 ns, with a shorter component of 5.0 ± 0.3 ns and a major

COMMUNICATION

contribution of a longer component of 23 ± 2 ns. The different lifetimes might be due to the presence of a flexible conformational system at the excited state^[10c] as it is the case of the different saddle-to-saddle conformers of **1** at the ground state.^[8b] No emission from triplet excited state could be observed up to 1650 nm even at low temperature 80 K.

Chiral resolution of **1** was achieved by chiral HPLC (see SI for details). Other diastereoisomers were not observed in HPLC traces during the enantiomeric resolution of **1**. Enantiopure **1** resulted configurationally stable showing a great stability to racemization as expected from the [7]helicene pitch difunctionalized in the fjord region^[19] with bulky ^tBu groups. Thus, neither racemization nor decomposition were observed by chiral HPLC after heating a hexadecane solution of enantiopure **1** at 180 °C for 24 h and then additional 4 h at 200 °C, which is in agreement with the described barrier of racemization of heptahelicene.^[20]

Electronic circular dichroism (ECD) spectra of both enantiomers were measured in CH₂Cl₂ and are presented in Figure 3 (top). Enantiopure **1** shows several Cotton effects along the UV-visible range, two main bisignated signals centered at 375 nm and 500 nm and a broad absorption band centered at 580 nm. The first HPLC fraction ($t_R = 5$ min) showed negative Cotton effect at 400 nm ($|\Delta\epsilon|$ of $112 \text{ M}^{-1} \text{ cm}^{-1}$, $g_{\text{abs}} = \Delta\epsilon/\epsilon = 2 \times 10^{-3}$) and at the lowest energy transition at 580 nm ($|\Delta\epsilon|$ of $43 \text{ M}^{-1} \text{ cm}^{-1}$, $g_{\text{abs}} = 2.5 \times 10^{-3}$). The second eluted enantiomer ($t_R = 6.5$ min) demonstrates a clear mirror image with positive Cotton effect at the longest wavelengths above 500 nm.

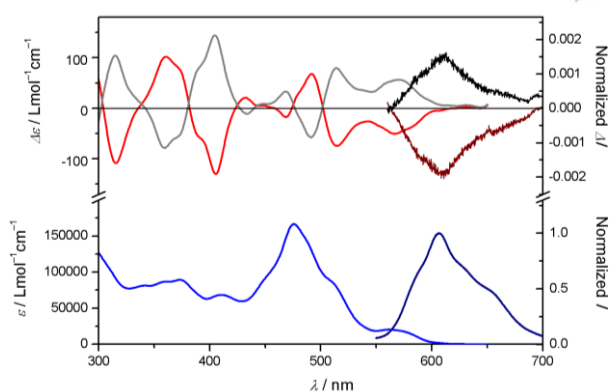


Figure 3. Top: Experimental ECD (left) and CPL (right, $\lambda_{\text{exc}} = 490$ nm) of (*M*) (red and wine) and (*P*) (grey and black) enantiomers of **1** in CH₂Cl₂ at ca. 5×10^{-6} M. Bottom: Experimental UV-vis (blue) and fluorescence (navy, $\lambda_{\text{exc}} = 490$ nm) of **1** in CH₂Cl₂ at ca. 5×10^{-6} M.

According with simulated ECD spectra of (*M*)-**1**, the first HPLC fraction corresponds with this enantiomer while the second fraction is assigned to the (*P*)-enantiomer (see SI, Figure S29). Hence, the sign of the ECD signal at the longest wavelength is consistent with that described for carbo[*n*]helicenes,^[21] and it also correlates with the sign of its CPL signal. As shown in Figure 3 (top right), CPL spectra were recorded for both enantiomers (*M*)-**1** and (*P*)-**1** at 10^{-6} M in CH₂Cl₂, thus avoiding any photoselection originated from the presence of aggregates. Upon irradiation with a blue light ($\lambda_{\text{exc}} = 490$ nm) mirror-shaped CPL spectra centered at 610 nm were obtained for both enantiomeric forms as expected

from a pure circularly polarized luminescence without any optical artifacts.^[22] The emission dissymmetry factor, g_{lum} , reached a value of 2×10^{-3} which represents a significant one order of magnitude increase in comparison with the unique nanographene reported as CPL emitter.^[8b] The dissymmetry factors relationship at 580 nm is $g_{\text{lum}}/g_{\text{abs}} = 0.8$,^[23] suggesting that the dissymmetry of **1** is mainly kept at the excited state, and that the $\pi\text{-}\pi^*$ electronic transition does not involve any important structural changes, as it is inherent to extended aromatics.

Cyclic voltammetry (CV) of **1** in THF shows two reversible oxidation and nine quasi-reversible reduction waves from -3 to +1.3 V (vs Fc/Fc⁺) (see SI, Figure S26). Squared-wave voltammetry (SWV) suggests the single-electron character of each redox process. This good electron accepting capability might find application as n-type materials in organic electronics or photovoltaic applications.^[24] HOMO-LUMO calculated from the first half-wave oxidation and reduction potentials resulted 2.33 eV, in the range of the optical band gap obtained from the curve crossing of the normalized absorption and emission spectra (2.20 eV) and also in good concordance with the DFT obtained value (2.6 eV).^[25]

Furthermore, the extended aromatic network of **1** favors the nonlinear absorption by simultaneous interaction with two photons in the NIR region. Excitation with a pair of degenerated photons in the 700-900 nm region using a femtosecond laser results in emission at higher energies (TPE at 550-700 nm in Figure 4, red circles). The upconverted emission (Figure 4, red line) overlaps with the one-photon induced emission spectrum (OPE in Figure 4, black line). The two-photon absorption (TPA) cross-section (σ_2) was calculated using the two-photon induced emission method (for more details see SI).^[26] A maximum σ_2 of 870 GM was estimated at ca. 800 nm corresponding to an overall transition energy of 400 nm. This value represents a 6.7-fold increase in comparison with the one recently reported for ribbon nanographene with push-pull character^[8b] or for carbon nanodots.^[27] The quadratic dependence of the TPE on the excitation power was confirmed by using different incident power (see SI, Fig. S22), and no net linear absorption was observed above 600 nm.

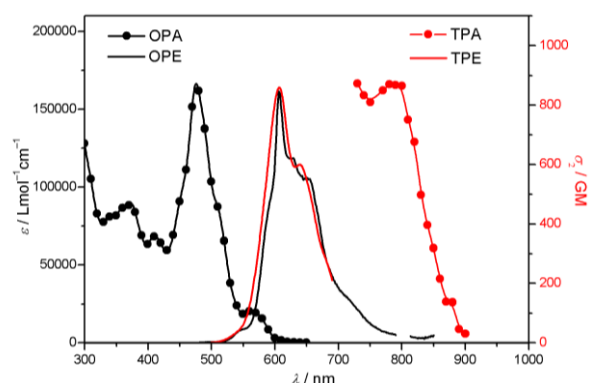


Figure 4. One- and two-photon absorption (OPA, black circles and TPA, red circles) and one and two-photon induced emission (OPE, black line, $\lambda_{\text{exc}} = 490$ nm and TPE, red line, $\lambda_{\text{exc}} = 800$ nm) of **1** in CH₂Cl₂ at ca. 1×10^{-6} M.

The helicene moiety does not usually exhibit good nonlinearity, however, remarkably TPA cross-section of **1** resulted two orders of magnitude higher than that reported for carbo[6]helicene.^[28] Thus, the expansion of the electronic delocalization beyond the helicene core improved the nonlinear optical responses as it has been reported for the case of hexa and heptahelicene derivatives.^[29]

The introduction of non-linear optics in chiral molecules, such as in the case of two-photon circular dichroism (TPCD), the non linear analogue of ECD, combines the advantages of both responses, minimizing linear absorption and scattering and giving relevant structural and conformational information of chiral frameworks.^[30] To the best of our knowledge, similar approach based on emission, namely two-photon circularly polarized luminescence (TPCPL) is yet to be developed and compound **1** represents a promising candidate for such approach.^[31] Both non-linear response (TPA) and chiral emission (CPL) are considerably improved in comparison with the sole example reported exhibiting both responses in a single molecule.^[8b] Although as a primary representative, helical nanographene strip **1** illustrates the demonstration of non-linear and chiroptical properties in graphene helicoidal which represents a promising field of research with a potential range of applications to be explored.^[32] Further work on CPL active distorted nanographenes is expected in the coming years as it might open a wide variety of applications for carbon nanoforms.

Acknowledgements

We acknowledge the European Research Council (ERC) under the European Union's Horizon 2020 research and innovation program (ERC-2015-STG-677023) and the Ministerio de Economía y Competitividad (MINECO, Spain) (CTQ2015-70283-P). C.M.C. and A.G.C. acknowledge contracts from MINECO (BES-2016-076371 and RyC-2013-12943). E.M. thank the Fundação para a Ciência e a tecnologia for financial support (UID/NAN/50024/2013 and IF/00759/2013). We thank the CSIRC-Alhambra for supercomputing facilities and the "Unidad de Excelencia Química Aplicada a Biomedicina y Medioambiente" both from the University of Granada.

Keywords: nanographenes • helicenes • circularly polarized luminescence • nanostructures • nonlinear optics

[1] K. Kim, Z. Lee, B. D. Malone, K. T. Chan, B. Alemán, W. Regan, W. Gannett, M. F. Crommie, M. L. Cohen, A. Zettl, *Phys. Rev. B* **2011**, *83*, 245433.
 [2] N. Yang, X. Ni, J.-W. Jiang, B. Li, *Appl. Phys. Lett.* **2012**, *100*, 093107.
 [3] a) J. Luo, X. Xu, R. Mao, Q. Miao, *J. Am. Chem. Soc.* **2012**, *134*, 13796-13803; b) A. Pradhan, P. Dechambenoit, H. Bock, F. Durola, *J. Org. Chem.* **2013**, *78*, 2266-2274; c) K. Kawasumi, Q. Zhang, Y. Segawa, L. T. Scott, K. Itami, *Nat. Chem.* **2013**, *5*, 739-744; d) K. Y. Cheung, X. Xu, Q. Miao, *J. Am. Chem. Soc.* **2015**, *137*, 3910-3914; e) K. Y. Cheung, C. K. Chan, Z. Liu, Q. Miao, *Angew. Chem. Int. Ed.* **2017**, *56*, 9003-9007; *Angew. Chem.* **2017**, *129*, 9131-9135; f) W. S. Wong, C. F. Ng, D. Kuck, H. F. Chow, *Angew. Chem. Int. Ed.* **2017**, *56*, 12356-12360; *Angew. Chem.* **2017**, *129*, 12528-12532; g) I. R. Márquez, N. Fuentes, C. M. Cruz, V. Puente-Muñoz, L. Sotorrios, M. L. Marcos, D. Choquesillo-

Lazarte, B. Biel, L. Croveto, E. Gómez-Bengo, M. T. González, R. Martín, J. M. Cuerva, A. G. Campaña, *Chem. Sci.* **2017**, *8*, 1068-1074.
 [4] a) I. R. Márquez, S. Castro-Fernández, A. Millán, A. G. Campaña, *Chem. Commun.* **2018**, 54, 6705-6718; (b) S. H. Pun, Q. Miao, *Acc. Chem. Res.* **2018**, DOI: 10.1021/acs.accounts.8b00140.
 [5] H. Zhan, G. Zhang, C. Yang, Y. Gu, *J. Phys. Chem. C* **2018**, *122*, 7605-7612.
 [6] H. Zhan, Y. Zhang, C. Yang, G. Zhang, Y. Gu, *Carbon* **2017**, *120*, 258-264.
 [7] F. Xu, H. Yu, A. Sadzadeh, B. I. Yakobson, *Nano Lett.* **2016**, *16*, 34-39.
 [8] a) T. Fujikawa, Y. Segawa, K. Itami, *J. Am. Chem. Soc.* **2015**, *137*, 7763-7768; b) C. M. Cruz, I. R. Márquez, I. F. A. Mariz, V. Blanco, C. Sánchez-Sánchez, J. M. Sobrado, J. A. Martín-Gago, J. M. Cuerva, E. Maçôas, A. G. Campaña, *Chem. Sci.* **2018**, *9*, 3917-3924; c) D. Reger, P. Haines, F. W. Heinemann, D. M. Guldi, N. Jux, *Angew. Chem. Int. Ed.* **2018**, *57*, 5938-5942; d) P. J. Evans, J. Ouyang, L. Favereau, J. Crassous, I. Fernández, J. Perles, N. Martín, *Angew. Chem. Int. Ed.* **2018**, *57*, 6774-6779; *Angew. Chem.* **2018**, *130*, 6890-6895; e) N. J. Schuster, R. Hernández Sánchez, D. Bukharina, N. A. Kotov, N. Berova, F. Ng, M. L. Steigerwald, C. Nuckolls, *J. Am. Chem. Soc.* **2018**, *140*, 6235-6239.
 [9] a) F. Zinna, L. Di Bari, *Chirality* **2015**, *27*, 1-13; b) E. M. Sánchez-Carnero, A. R. Agarrabeitia, F. Moreno, B. L. Maroto, G. Muller, M. J. Ortiz, S. de la Moya, *Chem. Eur. J.* **2015**, *21*, 13488-13500; c) J. Kumar, T. Nakashima, T. Kawai, *J. Phys. Chem. Lett.* **2015**, *6*, 3445-3452; d) G. Longhi, E. Castiglioni, J. Koshoubu, G. Mazzeo, S. Abbate, *Chirality* **2016**, *28*, 696-707.
 [10] a) H. Maeda, Y. Bando, K. Shimomura, I. Yamada, M. Naito, K. Nobusawa, H. Tsumatori, T. Kawai, *J. Am. Chem. Soc.* **2011**, *133*, 9266-9269; b) N. Saleh, B. Moore, 2nd, M. Srebro, N. Vanthuyne, L. Toupet, J. A. Williams, C. Roussel, K. K. Deol, G. Muller, J. Autschbach, J. Crassous, *Chem. Eur. J.* **2015**, *21*, 1673-1681; c) S. P. Morcillo, D. Miguel, L. Álvarez de Cienfuegos, J. Justicia, S. Abbate, E. Castiglioni, C. Bour, M. Ribagorda, D. J. Cárdenas, J. M. Paredes, L. Croveto, D. Choquesillo-Lazarte, A. J. Mota, M. C. Carreño, G. Longhi, J. M. Cuerva, *Chem. Sci.* **2016**, *7*, 5663-5670; d) S. Resa, D. Miguel, S. Guisán-Ceinos, G. Mazzeo, D. Choquesillo-Lazarte, S. Abbate, L. Croveto, D. J. Cárdenas, M. C. Carreño, M. Ribagorda, G. Longhi, A. J. Mota, L. Álvarez de Cienfuegos, J. M. Cuerva, *Chem. Eur. J.* **2018**, *24*, 2653-2662; e) K. Takaishi, M. Yasui, T. Ema, *J. Am. Chem. Soc.* **2018**, *140*, 5334-5338.
 [11] P. Reiné, J. Justicia, S. P. Morcillo, S. Abbate, B. Vaz, M. Ribagorda, Á. Orte, L. Álvarez de Cienfuegos, G. Longhi, A. G. Campaña, D. Miguel, J. M. Cuerva, *J. Org. Chem.* **2018**, *83*, 4455-4463.
 [12] a) Y. Yang, R. C. da Costa, M. J. Fuchter, A. J. Campbell, *Nat. Photon.* **2013**, *7*, 634-638; b) M. Li, S. H. Li, D. Zhang, M. Cai, L. Duan, M. K. Fung, C. F. Chen, *Angew. Chem. Int. Ed.* **2018**, *57*, 2889-2893; *Angew. Chem.* **2018**, *130*, 2939-2943.
 [13] a) M. Buchta, J. Rybáček, A. Jančařík, A. A. Kudale, M. Buděšínský, J. V. Chocholoušová, J. Vacek, L. Bednárová, I. Čísařová, G. J. Bodwell, I. Starý, I. G. Stará, *Chem. Eur. J.* **2015**, *21*, 8910-8917; b) Y. Hu, X. Y. Wang, P. X. Peng, X. C. Wang, X. Y. Cao, X. Feng, K. Müllen, A. Narita, *Angew. Chem. Int. Ed.* **2017**, *56*, 3374-3378; *Angew. Chem.* **2017**, *129*, 3423-3427; c) Y. Nakakuki, T. Hirose, H. Sotome, H. Miyasaka, K. Matsuda, *J. Am. Chem. Soc.* **2018**, *140*, 4317-4326; d) Y. Zhu, Z. Xia, Z. Cai, Z. Yuan, N. Jiang, T. Li, Y. Wang, X. Guo, Z. Li, S. Ma, D. Zhong, Y. Li, J. Wang, *J. Am. Chem. Soc.* **2018**, *140*, 4222-4226; e) R. Yamano, Y. Shibata, K. Tanaka, *Chem. Eur. J.* **2018**, *24*, 6364-6370.
 [14] M. Daigle, D. Miao, A. Lucotti, M. Tommasini, J.-F. Morin, *Angew. Chem. Int. Ed.* **2017**, *56*, 6213-6217; *Angew. Chem.* **2017**, *129*, 6309-6313.
 [15] Other fractions of mixtures of partially dehydrogenated compounds are also obtained as it is observed by mass spectrometry.
 [16] Single crystals of **1** were grown from methanol/chloroform mixtures. Unfortunately, X-ray diffraction measurements even with a synchrotron radiation source did not afford any useful results due to the small size of the crystal obtained.

- [17] M. Joly, N. Defay, R. H. Martin, J. P. Declercq, G. Germain, B. Soubrier-Payen, M. V. Meerssche, *Helv. Chim. Acta* **1977**, *60*, 537-560.
- [18] E. V. Donckt, J. Nasielski, *Chem. Phys. Lett.* **1968**, *2*, 409-410.
- [19] P. Ravat, R. Hinkelmann, D. Steinebrunner, A. Prescimone, I. Bodoky, M. Juriček, *Org. Lett.* **2017**, *19*, 3707-3710.
- [20] a) R. H. Martin, M. J. Marchant, *Tetrahedron* **1974**, *30*, 347-349; b) R. H. Janke, G. Haufe, E.-U. Würthwein, J. H. Borkent, *J. Am. Chem. Soc.* **1996**, *118*, 6031-6035.
- [21] F. Furche, R. Ahlrichs, C. Wachsmann, E. Weber, A. Sobanski, F. Vögtle, S. Grimme, *J. Am. Chem. Soc.* **2000**, *122*, 1717-1724.
- [22] Circularly polarization was also confirmed by looking at the signal at a frequency of $2 \times$ the frequency of the PEM acting as an oscillating quarter-wave plate: a) H. P. J. M. Dekkers, P. F. Moraal, J. M. Timper, J. P. Riehl, *Appl. Spectrosc.* **1985**, *39*, 818-821; b) J. P. Riehl, F. S. Richardson, *Chem. Rev.* **1986**, *86*, 1-16.
- [23] H. Tanaka, Y. Inoue, T. Mori, *ChemPhotoChem* **2018**, *2*, 386-402.
- [24] a) B. C. Thompson, J. M. Fréchet, *Angew. Chem. Int. Ed.* **2008**, *47*, 58-77; b) J. L. Delgado, P. -A. Bouit, S. Filippone, M. A. Herranz, N. Martín, *Chem. Commun.* **2010**, *46*, 4853-4865; c) J. E. Anthony, A. Facchetti, M. Heeney, S. R. Marder, X. Zhan, *Adv. Mater.* **2010**, *22*, 3876-3892.
- [25] G. Zhang, C. B. Musgrave, *J. Phys. Chem. A* **2007**, *111*, 1554-1561.
- [26] a) G. Marcelo, S. Pinto, T. Cañeque, I. F. A. Mariz, A. M. Cuadro, J. J. Vaquero, J. M. G. Martinho, E. M. S. Maçôas, *J. Phys. Chem. A* **2015**, *119*, 2351-2362; b) S. Reguardati, J. Pahapill, A. Mikhailov, Y. Stepanenko, A. Rebane, *Opt. Express* **2016**, *24*, 9053-9066.
- [27] C. I. M. Santos, I. F. A. Mariz, S. N. Pinto, G. Gonçalves, I. Bdiqin, P. A. A. P. Marques, M. Graça, P. M. S. Neves, J. M. G. Martinho, E. M. S. Maçôas, *Nanoscale* **2018**, *10*, 12505-12514.
- [28] Y. Vesga, C. Diaz, J. Crassous, F. E. Hernandez, *J. Phys. Chem. A* **2018**, *122*, 3365-3373.
- [29] C. Diaz, Y. Vesga, L. Echevarria, I. G. Stará, I. Starý, E. Anger, C. Shen, M. El Sayed Moussa, N. Vanthuyne, J. Crassous, A. Rizzo, F. E. Hernández, *RSC Adv.* **2015**, *5*, 17429-17437.
- [30] a) T. Verbiest, S. V. Elshocht, M. Kauranen, L. Hellemans, J. Snauwaert, C. Nuckolls, T. J. Katz, A. Persoons, *Science* **1998**, *282*, 913-915; b) P. Fischer, F. Hache, *Chirality* **2005**, *17*, 421-437.
- [31] A related process of CPL through triplet-triplet annihilation-based upconversion has been described: a) J. Han, P. Duan, X. Li, M. Liu, *J. Am. Chem. Soc.* **2017**, *139*, 9783-9786; b) P. Duan, D. Asthana, T. Nakashima, T. Kawai, N. Yanai, N. Kimizuka, *Faraday Discuss.* **2017**, *196*, 305-316.
- [32] J. R. Brandt, F. Salerno, M. J. Fuchter, *Nat. Rev. Chem.* **2017**, *1*, 0045.

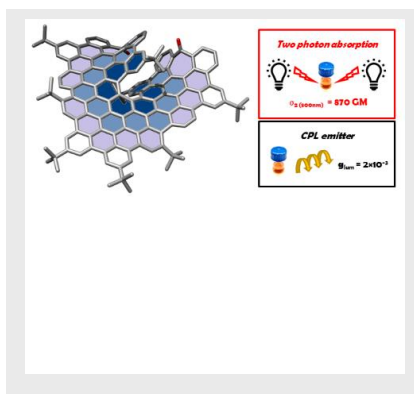
COMMUNICATION

Entry for the Table of Contents

Layout 1:

COMMUNICATION

A twist in the ribbon: a chiral helical nanographene with a central [7]helicene has been synthesized and both enantiomers isolated and studied. This first undecabenz[7]superhelicene exhibits remarkable chiroptical and non-linear optical properties.



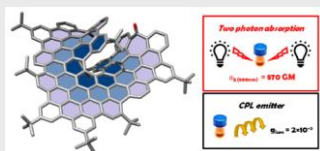
C. M. Cruz, S. Castro-Fernández, E. Maçôas, J. M. Cuerva, A. G. Campaña*

1 – 5

Undecabenz[7]superhelicene: a helical nanographene ribbon as CPL emitter

Layout 2:

COMMUNICATION



C. M. Cruz, S. Castro-Fernández, E. Maçôas, J. M. Cuerva, A. G. Campaña*

1 – 5

Undecabenz[7]superhelicene: a helical nanographene ribbon as CPL emitter

A twist in the ribbon: a chiral helical nanographene with a central [7]helicene has been synthesized and both enantiomers isolated and studied. This first undecabenz[7]superhelicene exhibits remarkable chiroptical and non-linear optical properties.